An investigation of the sodium patterning in Na_xCoO_2 ($0.5 \leqslant x \leqslant 1$) by density functional theory methods

Ying S. Meng,[1,a)] Yoyo Hinuma,[2] and Gerbrand Ceder[2]
[1]*Department of Materials Science and Engineering, University of Florida, 135 Rhines Hall, Gainesville, Florida 32611, USA*
[2]*Department of Materials Science and Engineering, Massachusetts Institute of Technology, 77 Massachusetts Avenue, Cambridge, Massachusetts 02139, USA*

(Received 26 October 2007; accepted 8 January 2008; published online 14 March 2008)

Extensive experimental work has been carried out to characterize the stable Na-vacancy ordering patterns at various compositions of layered Na_xCoO_2. However, contradictions and debates prevail in the literature, particularly at high Na concentrations $x>0.5$. Understanding of the exotic electronic properties in this system requires a thorough understanding of the Na-vacancy structural orderings. Using density functional theory in the generalized gradient approximation (GGA), combined with a cluster expansion structure prediction algorithm we have found an intricate set of Na-vacancy ordered ground states in Na_xCoO_2 ($0.5 \leqslant x \leqslant 1$). We demonstrate a newly predicted ordering pattern between $0.67 \leqslant x \leqslant 0.71$. By comparing the first principles electronic structure methods within the GGA and GGA+U (Hubbard U correction) approximations, we demonstrate that at certain Na concentration the stable ordering is affected by charge localization on the Co layer through coupling between the Na and Co lattices. © *2008 American Institute of Physics*. [DOI: 10.1063/1.2839292]

INTRODUCTION

The exceptional magnetic and electronic properties of sodium cobaltate (Na_xCoO_2) make it a material of great interest. At high sodium concentration it displays a remarkable combination of high electronic conductivity and high Seebeck coefficient,[1] while at low sodium content the hydrated form of the material is superconducting.[2] A recent 40-fold enhancement of the thermopower in Na_xCoO_2 ($x>0.75$) has revitalized its potential for thermoelectric applications.[3] The structure of these materials is particularly important as mixed Co^{3+}/Co^{4+} systems are often on the verge of a localization/delocalization transition,[4] and minor deviations of the local electrostatic potential on the Co site, such as those induced by local Na^+ order or disorder, may therefore significantly influence the electronic state. In this paper, we show, using first principles computations, that Na-vacancy ordering is complex and follows three distinct patterns depending on the Na content. Several new ground states are predicted, and we offer an explanation for the two-phase state that is often observed at composition $Na_{0.75}CoO_2$.

The structure of Na_xCoO_2 consists of Na layers stacked between layers of edge-sharing CoO_6 octahedra, as shown in Fig. 1. The close-packed oxygen ions stack as $ABBA|ABBA$,[5] with the oxygen ions on each side of the Na layer directly facing each other. This type of stacking leads to two types of prismatic sites for the Na ions: the oxygen prism around the Na(1) site shares a face with a CoO_6 octahedron above and below, while the prism around the Na(2) site only shares edges with adjacent CoO_6 octahedra. Together, the Na(1) and Na(2) sites form a triangular lattice. Figure 1(b) shows the projected view of the structure along the c_{hex} axis, revealing that the Na(2) sites in two adjacent layers are shifted due to the P2 ($AABB$) stacking of oxygen ions [Fig. 1(a)]. Though one might suspect the Na(1) site to be less favorable due to the stronger electrostatic repulsion from the Co ions, simultaneous occupation of Na(1) and Na(2) can result in larger average Na–Na distances than if only Na(2) sites are occupied. The complexity of Na-vacancy ordering in this system arises in part from this competition between the Na(1)–Na(2) site energy difference and the Na^+–Na^+ electrostatic repulsion. Experiments[6,7] and calculations[8] agree that the ordering pattern at $x=0.50$ (1/2) is the one shown in Fig. 2(b) with equal occupation of Na(1) and Na(2) sites. Extensive experimental and computational investigations have been carried out in finding the stable sodium-vacancy orderings at various other Na concentrations.[7,9,10] In a detailed electron diffraction study

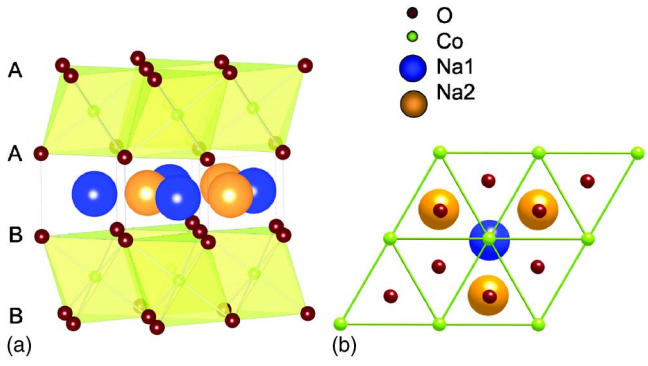

FIG. 1. (Color online) Crystal structure of P2-Na_xCoO_2. (a) View perpendicular to the c_{hex} to show the $AABB$ oxygen stacking. (b) View parallel to the c_{hex} to show relative positions of Na(1) and Na(2).

a)Electronic mail: ysmeng@mit.edu.

 © 2008 American Institute of Physics

Downloaded 06 Jun 2011 to 137.110.115.65. Redistribution subject to AIP license or copyright; see http://jcp.aip.org/about/rights_and_permissions

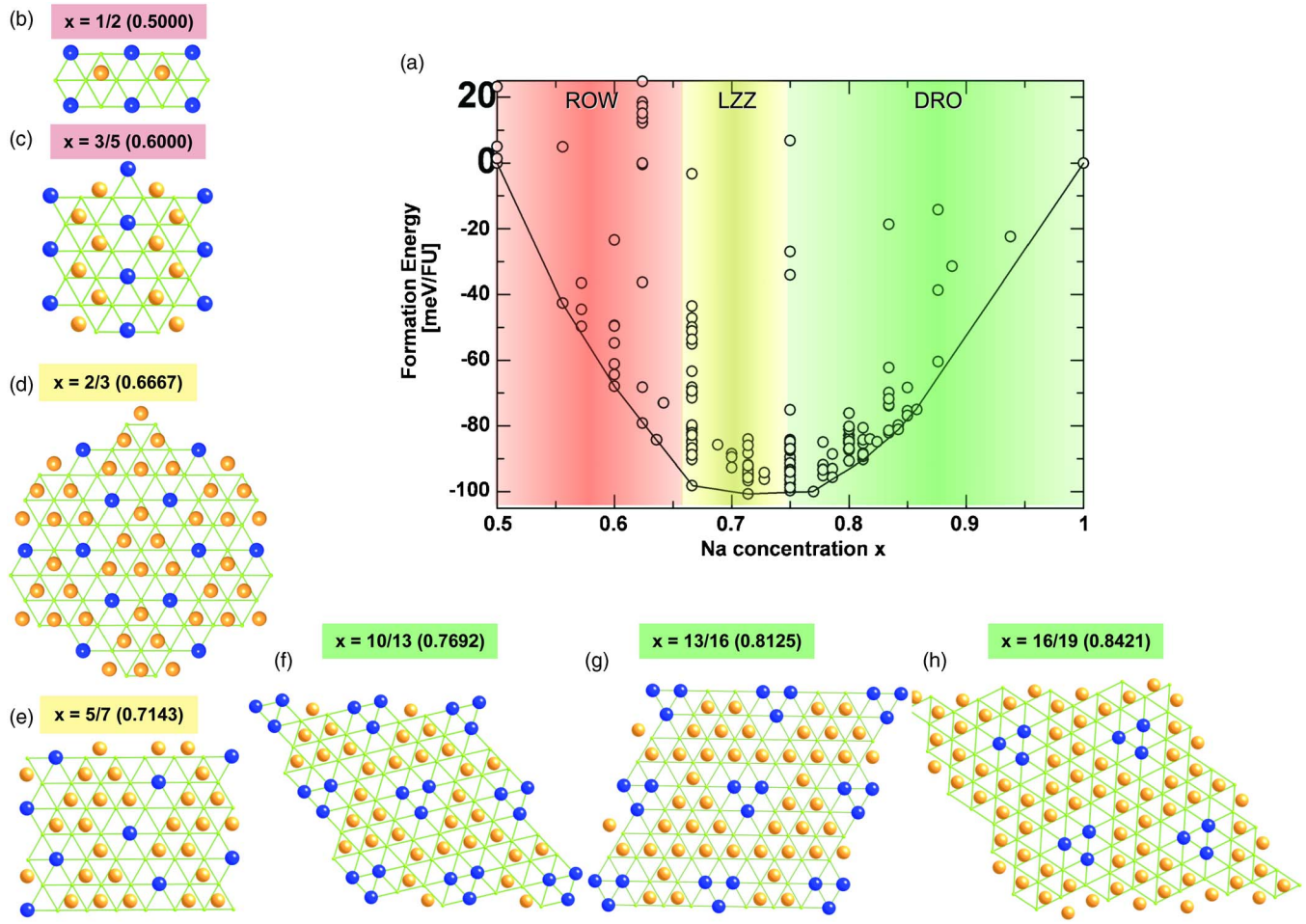

FIG. 2. (Color online) GGA formation energies of various Na-vacancy ordered states in P2-Na_xCoO_2 with some of the ground state structures shown. (a) The concentration range, where each of the three ordering patterns (ROW, LZZ, and DRO) are favored, are shaded in red, yellow, and green, respectively; ROW ordering occurs at (b) $x=1/2$ and (c) $x=3/5$; LZZ ordering occurs at (d) $x=2/3$ and (e) $x=5/7$; DRO ordering occurs at concentration $\geqslant 0.75$, e.g., (f) $x=10/13$, (g) 13/16, and (h) 16/19.

on powder samples, Zandbergen *et al.*[7] proposed several new structures including one at $x=0.75$. Though this structure was later also found in an *ab initio* study by Zhang *et al.*[8] using the local density approximation (LDA) to density functional theory (DFT) method, more recent computational[11,12] and experimental studies[9] suggested several different ordering patterns at $x=0.75$. While Zhang *et al.* also proposed new ground states at $x=0.60$ (3/5), 0.80 (4/5), and 0.83 (5/6), their computational search was limited to patterns that could fit in small unit cells. Most recently, Roger *et al.* applied single crystal neutron diffraction[10] to show that at large Na concentration, the Na-vacancy organizational principle is the stabilization of droplets of Na(1) occupation that are long-range ordered at some simple fractional concentrations, such as 0.75 (3/4) and 0.80 (4/5). They proposed an unusual series of ordering patterns where tri-Na(1) droplets are long-range ordered when the Na concentration exceeds 0.75.

Here we present a first principles study of the sodium-vacancy ordering in Na_xCoO_2 ($0.5 \leqslant x \leqslant 1.0$) using the GGA approximation to DFT. To search for ground states the energies of more than 210 structures are calculated. Structure candidates are taken from both experimental data as well as structures generated by a cluster expansion approach which can suggest from already calculated structures what other possible ground states may be.[13–21] This set includes many structures with very large unit cells, as well as the droplet phases suggested by Roger *et al.*[10] By using the cluster expansion method,[13,22–24] it has been possible to rather exhaustively search for a stable structure in this system. As a result, several new ground state structures have been identified.

COMPUTATIONAL METHODS

Calculations on various ordering arrangements were performed in the spin-polarized generalized gradient approximation to density functional theory. Core electron states were represented by the projector augmented-wave method[25] as implemented in the Vienna *ab initio* simulation package (VASP).[26] The Perdew-Burke-Ernzerhof exchange correlation[27] and a plane wave representation for the wavefunction with a cutoff of 450 eV were used. The Brillouin zone was sampled with a mesh including the gamma point. The density of the mesh for all calculations is approximately one point per 0.01 $Å^{-3}$. All unit cells are fully relaxed.

A smaller set of structures was calculated in the generalized gradient approximation with Hubbard U correction to DFT (GGA+U). The effective U value for Co is 5 eV in the Liechtenstein scheme.[28] This value of U is between the val-

Downloaded 06 Jun 2011 to 137.110.115.65. Redistribution subject to AIP license or copyright; see http://jcp.aip.org/about/rights_and_permissions

ues of $U=4.91$ eV for Co^{3+} and $U=5.37$ eV for Co^{4+} obtained with first principles perturbation theory in Li_xCoO_2,[29] and is consistent with the previous work on $Na_{0.75}CoO_2$.[11] The U correction is needed to correct for the self-interaction error on transition metals in DFT.

The cluster expansion method is used to search iteratively for new ground states to be computed with DFT. This methodology is well established for alloys,[13–21] and has previously been used to study Li-vacancy disorder in similar systems such as Li_xCoO_2,[22,23,30] Li_xNiO_2,[31] and $Li_xNi_{0.5}Mn_{0.5}O_2$.[32,33] In the GGA model, d states on Co delocalize and all Co have similar charge, even in the mixed valence regime. As a result, the configurational state of Na sites can be described by a lattice model, with variables describing whether Na or a vacancy sits on each site. The essential idea of the cluster expansion is then to expand the energy of the system in terms of these variables. Using the occupation variables $\sigma=1$ for Na and $\sigma=-1$ for vacancies for Na sites, the Hamiltonian becomes

$$E_V^{\text{predict}} = C + \sum_{i\in \text{Na 1 site}} V^{\text{Na 1}}\sigma_i + \sum_{i\in \text{Na 2 site}} V^{\text{Na 2}}\sigma_i + \sum_{i,j} V^{ij}\sigma_i\sigma_j + \sum_{i,j,k} V^{ijk}\sigma_i\sigma_j\sigma_k + \cdots . \quad (1)$$

Here, C is a constant and V are the effective cluster interactions. The energy difference of Na on Na(1) and Na(2) sites, averaged over all possible occupations surrounding the sites, is $2(V^{\text{Na1}}-V^{\text{Na2}})$. The indices i, j, and k are labels of sites in the cluster. Once Eq. (1) is parametrized by fitting it to a series of calculated energies of different structures, it can be used to search rapidly for potentially lower energy states with Monte Carlo techniques. The energies of these suggested new ground states are then calculated with DFT and the fitting process of Eq. (1) can be iterated until no new ground states are found.

In the GGA+U approximation, the additional problem of organizing charge occupancy on the Co sublattice appears, and the Na/vacancy and Co^{3+}/Co^{4+} sublattices interact with each other. Such a system with two partially disordered sublattices which interact with each other can be studied with a coupled cluster expansion.[34–36] A coupled cluster expansion is essentially an expansion in the product basis of the configurational functions (clusters) defined on each sublattice.[37] A similar approach was recently used to capture the interaction between disorder of Li/vacancy and Fe^{2+}/Fe^{3+} disorder in Li_xFePO_4.[35] The GGA+U cluster expansion Hamiltonian becomes

$$E_V^{\text{predict}} = C + \sum_{i\in \text{Na 2 site}} V^{\text{Na 2}}\sigma_i + \sum_{i\in \text{Co site}} V^{\text{Co}}\tau_i + \sum_{i,j} V^{ij}\sigma_i\sigma_j + \sum_{i,j} V^{ij}\sigma_i\tau_j + \sum_{i,j} V^{ij}\tau_i\tau_j + \sum_{i,j,k} V^{ijk}\sigma_i\sigma_j\sigma_k + \sum_{i,j,k} V^{ijk}\sigma_i\sigma_j\tau_k + \sum_{i,j,k} V^{ijk}\sigma_i\tau_j\tau_k + \sum_{i,j,k} V^{ijk}\tau_i\tau_j\tau_k + \cdots , \quad (2)$$

where the occupation variables are $\sigma=1$ for Na and $\sigma=-1$ for vacancies at Na sites, and $\tau=1$ for Co^{3+} and $\tau=-1$ for Co^{4+} at Co sites.

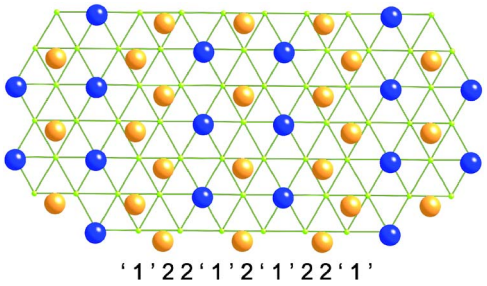

FIG. 3. (Color online) Na ordering at $x=5/9$ (0.5556). The pattern $\langle$'1'2'1'$2^2\rangle$ can be recognized as a combination of ordering at 2/4 (0.50) $\langle$'1'2$\rangle$ and 3/5 (0.60) $\langle$'1'$2^2\rangle$.

While in principle the expansion of Eqs. (1) and (2) has to be summed over all pairs, triplets, quadruplets, and larger clusters of sites, in practice relevant cluster interactions can be selected on the basis of how well they minimize the weighted cross-validation score, which is a means of measuring how good the cluster expansion is at predicting the energy of a structure not included in the fit.[38] This amounts to neglecting the effect of configurational details beyond a certain range on the energy. The final GGA cluster expansion was fitted to the energies of 211 different Na/vacancy configurations, and the final GGA+U cluster expansion was fitted to the energies of 131 different Na/vacancy and Co^{3+}/Co^{4+} configurations in the concentration range $0.5\leqslant x\leqslant 1$.

Grand canonical Monte Carlo simulations were conducted with this cluster expansion. Cooling calculations were conducted at fixed chemical potential to obtain the minimum energy $E-\mu x$ for different chemical potentials μ. Cells with up to approximately 30 000 Na sites (15 000 f.u.) were used. In the calculations 80 000 equilibrium passes and 120 000 sampling passes were used at 10 K intervals. One sampling pass amounts to one possible perturbation of each site on the lattice.

RESULTS AND DISCUSSIONS

Figure 2 shows the energies of the structures calculated for $0.5\leqslant x\leqslant 1$. The energy shown is the mixing energy with respect to the most stable structure at $x=0.5$ and $x=1$. The ground state structures are the vertices of the convex hull that defines the minimal energy as a function of composition. We find that there are three concentration ranges (color coded in Fig. 2) each with a distinct ordering motif in the ground states.

At $x=0.5(1/2)$, $x=0.56(5/9)$ (shown in Fig. 3), and $x=0.6(3/5)$ Na orders in rows either on Na(1) or on Na(2) sites. The structure at $x=0.5$, which has already been proposed previously,[6,7] has equal occupancies of Na(1) and Na(2) as it minimizes the electrostatic energy by eliminating Na(1)–Na(1) or Na(2)–Na(2) nearest neighbor interactions. The ordered state where all Na atoms form zigzag lines on Na(2) sites, with no Na(1) sites occupied, has 23 meV/f.u. higher energy (1 f.u. contains one Co atom). So, while the ground state ordering has half of its Na on less favorable

Downloaded 06 Jun 2011 to 137.110.115.65. Redistribution subject to AIP license or copyright; see http://jcp.aip.org/about/rights_and_permissions

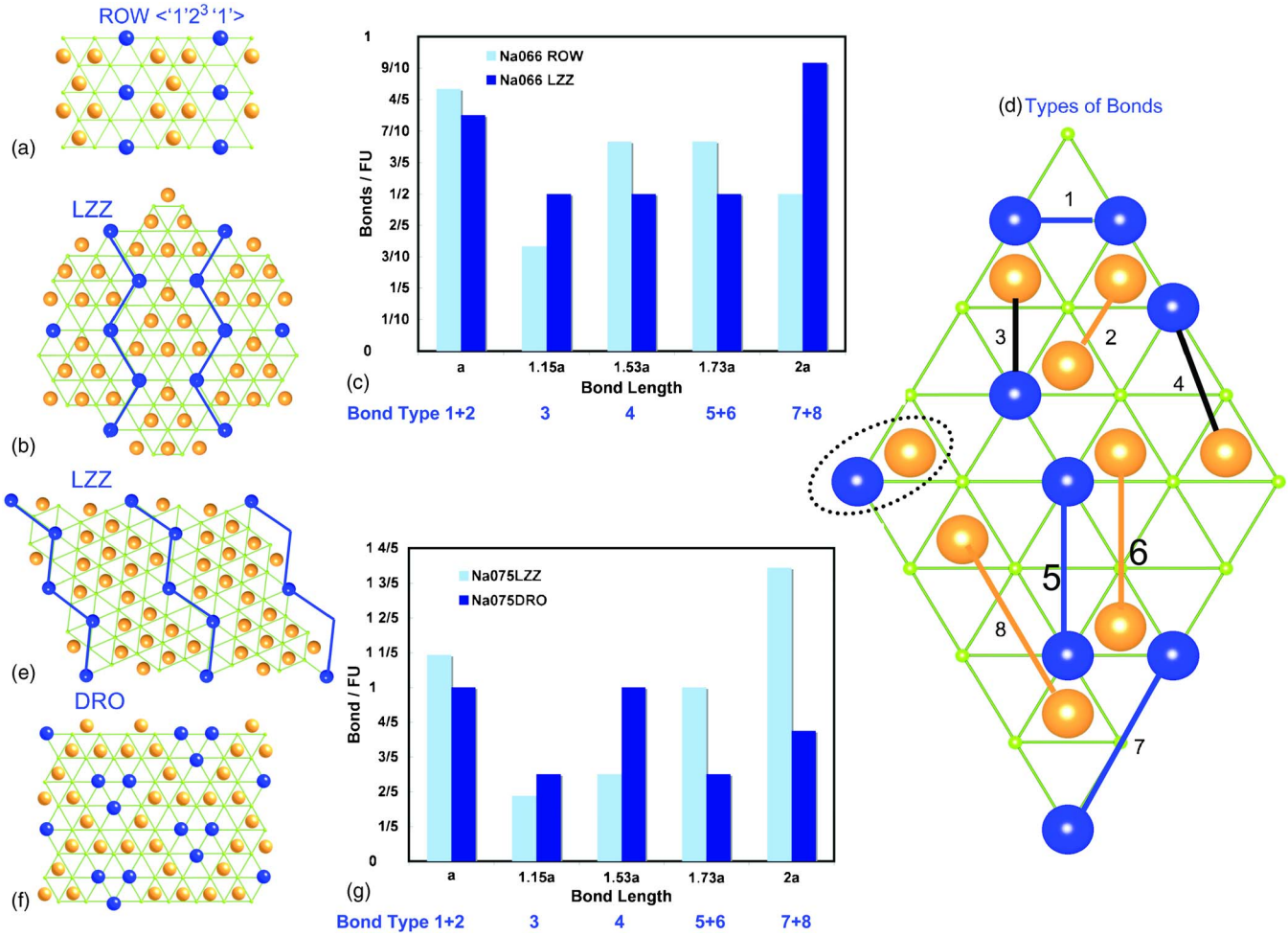

FIG. 4. (Color online) Average numbers of bonds per formula unit (Na_xCoO_2) for bond length up to $2a_{hex}$ for various ordering patterns. (a) ROW ordering pattern and (b) LZZ ordering pattern for $Na_{0.67}CoO_2$; (c) comparison for ROW and LZZ orderings for $x=0.67$; (d) types of bonds within $2a_{hex}$ (each type of bond is labeled and corresponds to the bond length in the histogram), the Na(1)–Na(2) nearest neighbor is circled with a dashed line since it never appears in any calculations. (e) LZZ ordering and (f) DRO ordering of $Na_{0.75}CoO_2$; (g) comparison of the number of bonds per formula unit (Na_xCoO_2) for band length up to $2a_{hex}$ in LZZ and DRO ordering for $x=0.75$.

sites [Na(1)] it gains stability by minimizing the electrostatic repulsions among Na ions. The ground state structure at 0.6 [Fig. 2(c)] is obtained from the one at $x=0.5$ by inserting an additional row of Na(2) ions between the Na(1) rows, creating some Na(2)–Na(2) nearest neighbors. Since the common characteristic of the ground states at $x=0.5$ and $x=0.6$ is the formation of rows of Na(1) and Na(2) ions, we can assume that these row motifs also occur at compositions $0.5<x<0.6$, which reduces the ground state problem in that concentration range to finding how the Na(1) and Na(2) rows alternate along the direction perpendicular to them. The ground states of such one-dimensional models are well known since the seminal work of Hubbard who found the ground states for arranging electrons and vacant sites on a one-dimensional lattice.[39] A similar analysis has been applied to explain the oxygen ordering in yttrium barium copper oxides.[40] Denoting by $\langle$'1'$\rangle$ a unit consisting of a row of Na(1) ions with a vacant row on each side and by $\langle 2\rangle$ a row of Na(2) ions, the ground states at $x=0.5$ and $x=0.6$ can be denoted as $\langle$'1'2$\rangle$ and $\langle$'1'$2^2\rangle$, respectively. For repulsive convex decaying interactions, typical for electrostatically interacting systems, there would be an infinite branching tree of ground states generated by a continued fraction algorithm, equivalent to a structure-combination branching mechanism.[41] For example, a new ground state would be expected at $(2+3)/(4+5)=5/9(0.5556)$, with Na ordering $\langle$'1'2'1'$2^2\rangle$ (see Fig. 3). Indeed, we calculated the energy of this structure with *ab initio* methods and found that it is lower than the compositionally weighted average of $\langle$'1'2$\rangle$ and $\langle$'1'$2^2\rangle$ structures. It is likely that the continued fraction algorithm leads to additional ground state structures (e.g., for $x=(2+5)/(4+9)=7/13$ and $(5+3)/(9+5)=8/14$) as is the case in $YBa_2Cu_3O_{7-\delta}$,[40] but the very large size of the unit cell precludes their energy calculations with DFT. While one could extend the ordering scheme for $x>0.6$, we will show in the subsequent section how the system "reorders" and finds a better solution to reduce the number of the nearest neighbor interactions.

The stable ordering patterns from $0.67(4/6)\leqslant x\leqslant 0.71(5/7)$ consist of Na(1) connecting in a zigzag pattern. The distance between such Na(1) ions is at least $2a_{hex}$; therefore the ordering scheme is named large zigzag (LZZ). The driving force for the change in pattern with increasing Na concentration can be rationalized if we compare the number

Downloaded 06 Jun 2011 to 137.110.115.65. Redistribution subject to AIP license or copyright; see http://jcp.aip.org/about/rights_and_permissions

of bonds in the $\langle$'1'$2^3\rangle$ [Fig. 4(a)] and LZZ [Fig. 4(b)] patterns for $x=2/3$ as a function of the distance [Fig. 4(c)]. All bonds within the distance $2a_{hex}$ are depicted on the triangular lattice in Fig. 4(d). One can see that the LZZ type of arrangement reduces the nearest neighbor bonds (a_{hex}) and those bonds at intermediate distance ($1.53a_{hex}$ and $1.73a_{hex}$), even though the numbers of the second nearest neighbor Na(1)–Na(2) bonds ($1.15a_{hex}$) and longer distance bonds ($2a_{hex}$) increase. Since a screened Columbic repulsion is more dominant for shorter bonds than longer bonds, the LZZ is expected to be more stable than $\langle$'1'$2^3\rangle$ since the two ordering patterns have the same Na(1)/Na(2) ratio. Indeed, in our *ab initio* calculations, the LZZ structure is 20 meV/f.u. lower in energy than the $\langle$'1'$2^3\rangle$ structure at $x=0.67$. For higher fraction of Na, such as $x=0.71(5/7)$, the distance between large zigzag lines is further expanded with more Na(2) ions inserted in between, as shown in Fig. 2(e).

While LZZ ordering can be constructed at $x=0.75(6/8)$ [Fig. 4(e)], one can again establish another ordering scheme to minimize the Na(1)–Na(1) and Na(2)–Na(2) nearest neighbor interactions, by forming ordered tri-Na(1) droplets shown in Fig. 4(f). One can see from the bond-counting histogram [Fig. 4(g)] that the droplet ordering has fewer bonds at $1.73a_{hex}$ and $2a_{hex}$ as well. The energy difference between these two ordering patterns is, however, only 1–2 meV/f.u. in GGA, probably because the droplet formation requires higher occupancy of Na(1) sites. Hence, at this composition the competition between Na(1)/Na(2) site energy and the Na^+–Na^+ repulsion brings very different ordering patterns close in energy. The long-range ordered patterns of tri-Na(1) droplets are found most stable in the concentration range $0.75<x<0.8571$ [Figs. 2(f)–2(h)]. At concentrations $x=0.7692(10/13)$, $0.8125(13/16)$, and $0.8421(16/19)$, we found stable structures in which tri-Na(1) droplets are maximally separated. The appearance of droplet phases in our *ab initio* calculation is in good agreement with the recent report of Roger *et al.* on the single crystal neutron diffraction observation of such ordering,[10] most recently confirmed by Wang and Ni's *ab initio* work.[12] Our cluster expansion extrapolation of the DFT data also predicts that sextet-Na(1) droplets could be the stable configuration when the Na concentration is approximately above 0.85. However, the size of this structure's unit cell (more than 200 atoms) prohibited a direct DFT calculation to verify this. One can, however, rationalize the stability of the sextet-Na(1) droplet by similar bond counting shown previously. In Fig. 5, we demonstrate that there is a reduction in energy at the dilute vacancy limit [high Na concentration ($x\sim1$)] when large Na(1) clusters are formed.

In order to directly compare the predicted physical properties with experimental values, we compare the calculated c lattice parameter for the ground states as a function of Na concentration to experimental values in Fig. 6. Since the growth mechanisms of single crystals and polycrystalline powders are different and often result in a slight difference in lattice parameters and degree of ordering, data from both types of samples are shown here. Our work agrees very well with polycrystalline powder measurement. A more subtle verification of the accuracy of our predictions can be made

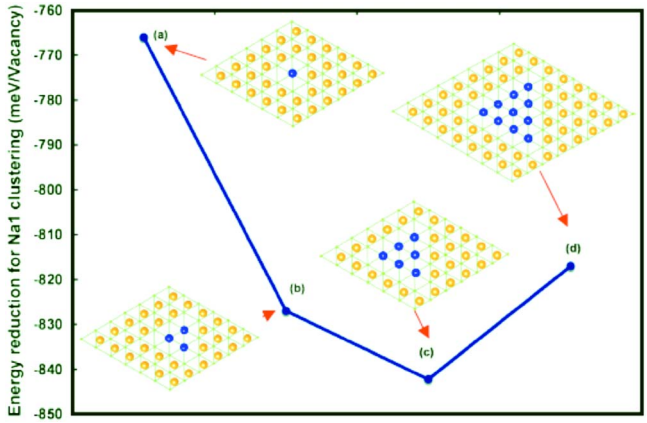

FIG. 5. (Color online) The stabilization energy of Na(1) cluster formation in the dilute vacancy limit. Decrease in energy per vacancy when Na in $NaCoO_2$ is replaced by vacancies in various environments where singlet, triplet, sextet, and decatet Na(1) droplets form. The concentration is at the dilute vacancy limit $x\approx1$, where there are no interactions between motifs. The energy change is calculated based on the changes in bonds between Na ions per vacancy up to distance $2a_{hex}$. The strength of the pair interactions is obtained with a cluster expansion. Details of the cluster expansion will be reported in a separate paper.

by comparing the Na(1)/Na(2) ratio measured by various experimental groups to our calculated results (Fig. 7) as this ratio depends more sensitively on the structure than the c lattice parameter does. The trend in our study, including the small dip around $x=0.71(5/7)$, is in good agreement with experiments[42–44] and agrees qualitatively well with Monte Carlo simulations by Roger *et al.*[10] on an electrostatic model. It is likely that our DFT results give slightly lower Na(1)/Na(2) values since DFT results are taken from ground state (0 K) structures, whereas experiments are at finite temperatures and the Na(1)/Na(2) disorder is known to increase with temperature.[45] Our results are in much better agreement with experimental data than previous DFT/LDA studies[8] where a less complete structural study was performed.

Our results may give some insight into the conflicting

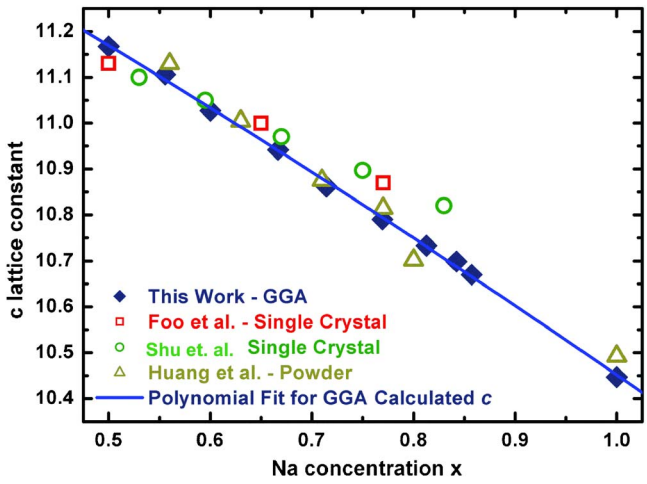

FIG. 6. (Color online) c lattice constant as a function of Na concentration. The open symbols show available experimental data from both the single crystal (Refs. 50 and 57) and powder diffraction (Ref. 42) measurements. The solid symbols are from our DFT calculations. A parabolic curve $c=-0.18785x^2-1.15505x+11.79412$ is fitted to the calculated values.

Downloaded 06 Jun 2011 to 137.110.115.65. Redistribution subject to AIP license or copyright; see http://jcp.aip.org/about/rights_and_permissions

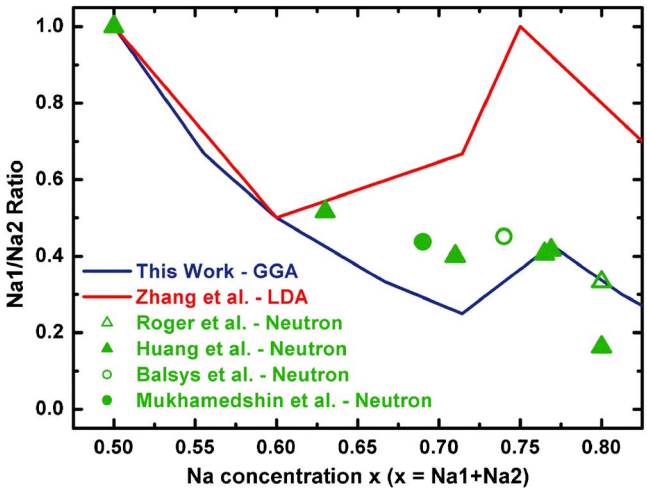

FIG. 7. (Color online) Change in Na(1)/Na(2) occupation ratio with Na concentration. The symbols show neutron data (Refs. 10 and 42–44). The red line shows the results obtained from previous DFT studies (Ref. 8). The blue line shows that our DFT calculation results are in good agreement with experiments, although the Na(1)/Na(2) ratio is from ground state calculations.

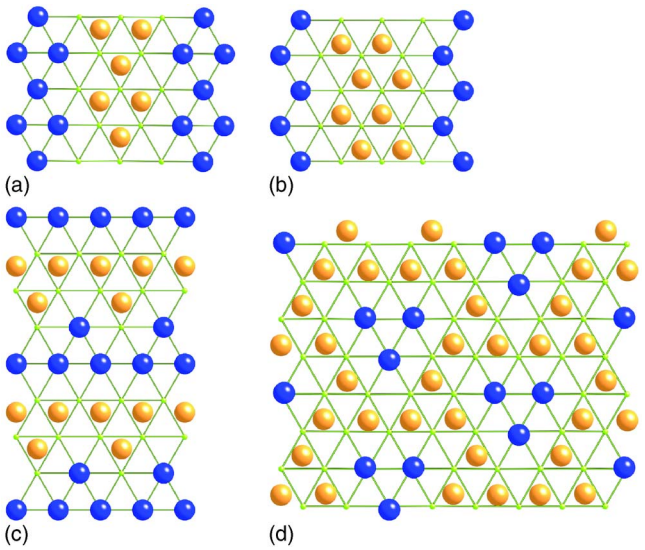

FIG. 8. (Color online) Ordering patterns at $x=3/4$ (0.75) proposed by (a) Ref. 7, named as "diamond," (b) Ref. 11, named as "zigzag," (c) Ref. 9, named as "stripe," (d) Ref. 10, named as "droplet."

experimental results reported for $x=0.75$. Powder neutron diffraction measurements by Huang *et al.*[42] suggest three different types of phases due to the Na ordering: H1, H2, and H3 phases in the range of $0.3<x<1$ with phase separation between H1 and H2 at $x=0.75$.[42] Zandbergen,[7] Geck,[9] and Meng[11] have all reported slightly different ordered structures for $x=0.75$. Given that $x=0.75$ is a simple rational concentration at which most systems actually order, phase separation may be at first surprising. However, our calculations confirm the lack of a stable ground state at $x=0.75$ due to the crossover of ordering patterns from LZZ-type ordered phases at $x=0.71(5/7)$ and the DRO-type phases starting at $x \geqslant 0.77(10/13)$, though it needs to be stated that the tri-Na(1) droplet ordering proposed by Roger *et al.*[10] [Fig. 4(f)] is only about 1 meV/f.u. above the two-phase state at $x=0.75$. Given the small energy differences between the phases, and the fact that around $x \approx 0.75$ the competition between the Na(1)–Na(2) site energy difference and the Na^+–Na^+ repulsion is almost perfectly in balance, leading to very different orderings with the same energy, it is possible that finite temperature or small compositional (in Na or impurities) changes lead to different structures. The diamond-type structure proposed by Zandbergen *et al.*[7] and calculated in Ref. 8, the stripe ordering proposed by Geck *et al.*,[9] and the zigzag ordering proposed by Meng *et al.*[11] (see Fig. 8) are all found to be only slightly higher in energy than the tri-Na(1) droplet ordering, giving $E_{\text{droplet}}<E_{\text{zigzag}}<E_{\text{stripe}}<E_{\text{diamond}}$ in both LDA and GGA. The LDA calculated energy for Fig. 8(d) E_{droplet} is the lowest, E_{zigzag} is 6 meV/f.u. higher, E_{stripe} is 12 meV/f.u. higher, and E_{diamond} is 17 meV/f.u. higher than E_{droplet}. In GGA calculations, E_{diamond}(+18 meV/f.u.)$>E_{\text{stripe}}$(+12 meV/f.u.)$>E_{\text{zigzag}}$(+7 meV/f.u.)$>E_{\text{droplet}}$ (0 meV/f.u., the reference state). The results are obtained for fully relaxed cells. In GGA+U calculations, the energy differences are larger due to the lock-in of Na-vacancy ordering by Co charge ordering: E_{diamond}(+26 meV/f.u.)$>E_{\text{zigzag}}$(+21 meV/f.u.)$>E_{\text{stripe}}$(+14 meV/f.u.)$>E_{\text{droplet}}$ (0 meV/f.u., the reference state). We notice that the energy sequence for Fig. 8(b) E_{zigzag} and Fig. 8(c) E_{stripe} is reversed in Ref. 12; however, the main conclusion that the droplet structure is the lowest in energy is consistent. Since the Na(1)/Na(2) ratio for both droplet and zigzag ordering is 1:2, in agreement with neutron diffraction refinement they seem to be the structural models most consistent with experiment. Both stripe and diamond structures have higher Na(1)/Na(2) ratio 1:1. In contrast to Refs. 8 and 12, the c lattice parameter is fully relaxed in our calculations. Indeed, when constraining the c lattice parameter we obtained the same results as previous reports[6,9,12] but different from the true energy minima, pointing at the critical role c lattice parameter relaxation plays in determining the ground state.

Two-phase regions are also observed experimentally in other concentration ranges. Nuclear magnetic resonance and x-ray diffraction results by Mukhamedshin *et al.* suggest the existence of four phases between $0.65<x<0.76$.[46] They found commensurate phases at $x\sim0.67$ and 0.75, and incommensurate phases at $x=0.70$–0.71 and 0.71–0.72. Carretta *et al.*[47] claimed magnetic phase separation at $x=0.65$, 0.70, and 0.75, which they believe is a consequence of rearrangement of Na ions when temperature decreases. Our first principles results offer a plausible explanation for the observations of these various two-phase regions, since we obtain ground states at $x=0.60$, 0.67, 0.71, and 0.77.

It is important to realize that standard exchange correlation approximations to DFT such as LDA and GGA treat the electronic structure as metallic, leading to all Co ions in the system being similar and of average valence. Whether such a delocalized electron state is more appropriate than discrete Co^{3+}/Co^{4+} has been under intense debate[46,48–52] and may depend on the Na concentration (and maybe even on the Na arrangement). In order to address the issue of how Na ordering patterns would be affected by charge localization (or the lack of it) in the CoO_2 layer, we have carried out GGA+U calculations. The +U approximation fully localizes the 3d

Downloaded 06 Jun 2011 to 137.110.115.65. Redistribution subject to AIP license or copyright; see http://jcp.aip.org/about/rights_and_permissions

TABLE I. Summary of ground states for Na_xCoO_2 $(0.5 \leqslant x \leqslant 1)$. (Values in parentheses are not used in Figs. 6 and 7 since their energies are not on the convex hull.)

	Ground state GGA	Ground state GGAU	Model	Na1/Na2 ratio GGA	c lattice GGA (Å)
0.5000 (1/2)	Y	Y	$\langle 1'2 \rangle$	1.0000	11.167
0.5556 (5/9)	Y	N	$\langle 1'2'1'2^2 \rangle$	0.6667	11.106
0.6000 (3/5)	Y	N	$\langle 1'2^2 \rangle$	0.5000	11.027
0.6667 (2/3)	Y	Y	LZZ	0.3333	10.942
0.7143 (5/7)	Y	N	LZZ	0.2500	10.862
0.7500 (3/4)	N	Y	DRO	(0.5000)	(10.828)
0.7692(10/13)	Y	N	DRO	0.4286	10.790
0.7857(11/14)	N	N	DRO	(0.3750)	(10.771)
0.8000(12/15)	N	N	DRO	(0.3333)	(10.752)
0.8125(13/16)	Y	N	DRO	0.3000	10.733
0.8235(14/17)	N	N	DRO	(0.2727)	(10.718)
0.8333(15/18)	N	N	DRO	(0.2500)	(10.708)
0.8421(16/19)	Y	N	DRO	0.2308	10.699
0.8500(17/20)	N	N	DRO	(0.2143)	(10.684)
0.8571(18/21)	Y	N	DRO	0.2000	10.670
1.0000 (1/1)	Y	Y	P2-$NaCoO_2$	0	10.447

states on Co for large enough U. We find that for $U=5$ eV, Co^{3+}/Co^{4+} can clearly be differentiated, as reported previously.[11,51,53] Although it is known that Na_xCoO_2 at $0.5<x<1$ is metallic, weak charge ordering at 0.5 and 0.75 has been reported.[54–56] We find that at $x=0.50$, 0.67, and 0.75, Co^{3+}/Co^{4+} charge ordering in our calculations can be stable only if the charge ordering is commensurate with that of the Na ordering pattern and the combined ordering minimizes the number of Na nearest neighbors to Co^{4+}. We find that GGA+U gives the same Na ordering patterns as in GGA at these compositions, but the ground states are much stronger (making the convexity of the energy hull larger) because of the energy associated with Co charge ordering. This means the charge ordering at simple fractions such as 1/2, 2/3, and 3/4 helps to lock-in and strengthens the Na orderings shown previously. Because the coupling between Co-charge ordering (on a triangular lattice) and the Na-vacancy ordering (on AB stacked triangular lattices below and above the Co layer) cannot easily be commensurated at arbitrary compositions, there are also fewer ground states in GGA+U compared to those in GGA (see Table I). For example, GGA+U makes the tri-Na(1) droplet phase absolutely stable at $x=0.75$ unlike in GGA where its energy is slightly higher than that of the two-phase state. Although GGA and GGA+U represent the two extreme scenarios where charges on the Co 3d states are, respectively, fully delocalized and statically localized, and the former approximation might be better suited for a Na_xCoO_2 $(x<1)$ ground state search, it is clear from comparing GGA to GGA+U results that even small amounts of charge localization may be enough to affect the Na ordering. This suggests that a very strong coupling exists between the electronic state and the Na-vacancy ordering.

CONCLUSIONS

In summary, using DFT methods we have found an intricate set of Na-vacancy ordered ground states in Na_xCoO_2. Three distinct ordering patterns are found with the transition between them occurring due to the balance between Na(1)–Na(2) site energies and electrostatic repulsion between Na^+ ions. The ground state structures at 0.50, 0.75, and 0.84, the c lattice parameter change, and the Na(1)/Na(2) ratio variation with sodium concentration are in excellent agreement with experimental observations. Between $0.66 \leqslant x \leqslant 0.71$ new "LZZ-ordered" states are predicted. Our results also shed some light on the phase separation in Na_xCoO_2 at high sodium concentration, $x>0.71$, and the coupling of Co charge localization to Na-vacancy ordering at simple fractions such as 0.67 (2/3) and 0.75 (3/4). Finally, our study indicates that disagreement between previous DFT calculations and experiments are largely due to the model assumptions unrelated to the accuracy of DFT, so that DFT can be reconsidered as a tool for understanding the complex sodium ordering structures in Na_xCoO_2.

ACKNOWLEDGMENTS

This work was supported by the U.S. Department of Energy, Office of Basic Energy Sciences under Contract No. DE-FG02-96ER-45571. The authors thank the National Partnership for Advanced Computational Infrastructure (NPACI) for computing time. Y.S.M. thanks A. Van der Ven and D. Carlier for fruitful discussion. Y.H. thanks T. Mueller and A. Van der Ven for the cluster expansion and Monte Carlo simulation codes.

[1] I. Terasaki, Y. Sasago, and K. Uchinokura, Phys. Rev. B **56**, 12685 (1997).
[2] K. Takada, H. Sakurai, E. Talcayama-Muromachi, F. Izumi, R. A. Dilanian, and T. Sasaki, Nature (London) **422**, 53 (2003).
[3] M. Lee, L. Viciu, L. Li, Y. Wang, M. L. Foo, S. Watauchi, R. A. Pascal, R. J. Cava, and N. P. Ong, Nat. Mater. **5**, 537 (2006).
[4] M. Ménétrier, I. Saadoune, S. Levasseur, and C. Delmas, J. Mater. Chem. **9**, 1135 (1999).
[5] C. Delmas, J. I. Braconnier, C. Fouassier, and P. Hagenmuller, Solid State Ionics **3–4**, 165 (1981).

Downloaded 06 Jun 2011 to 137.110.115.65. Redistribution subject to AIP license or copyright; see http://jcp.aip.org/about/rights_and_permissions

[6] Q. Huang, M. L. Foo, J. W. Lynn, H. W. Zandbergen, G. Lawes, Y. Y. Wang, B. H. Toby, A. P. Ramirez, N. P. Ong, and R. J. Cava, J. Phys.: Condens. Matter **16**, 5803 (2004).
[7] H. W. Zandbergen, M. Foo, Q. Xu, V. Kumar, and R. J. Cava, Phys. Rev. B **70**, 024101 (2004).
[8] P. H. Zhang, R. B. Capaz, M. L. Cohen, and S. G. Louie, Phys. Rev. B **71**, 153102 (2005).
[9] J. Geck, M. von Zimmermann, H. Berger, S. V. Borisenko, H. Eschrig, K. Koepernik, M. Knupfer, and B. Buchner, Phys. Rev. Lett. **97**, 106403 (2006).
[10] M. Roger, D. J. P. Morris, D. A. Tennant, M. J. Gutmann, J. P. Goff, J. U. Hoffmann, R. Feyerherm, E. Dudzik, D. Prabhakaran, A. T. Boothroyd, N. Shannon, B. Lake, and P. P. Deen, Nature (London) **445**, 631 (2007).
[11] Y. S. Meng, A. Van der Ven, M. K. Y. Chan, and G. Ceder, Phys. Rev. B **72**, 172103 (2005).
[12] Y. Wang and J. Ni, Phys. Rev. B **76**, 094101 (2007).
[13] I. M. Sanchez, F. Ducastelle, and D. Gratias, Physica A **128**, 334 (1984).
[14] D. de Fontaine, Solid State Phys. **47**, 33 (1994).
[15] G. Ceder, A. Van der Ven, C. Marianetti, and D. Morgan, Modell. Simul. Mater. Sci. Eng. **8**, 311 (2000).
[16] M. Asta, S. M. Foiles, and A. A. Quong, Phys. Rev. B **57**, 11265 (1998).
[17] C. Wolverton, Philos. Mag. Lett. **79**, 683 (1999).
[18] V. Ozolins, B. Sadigh, and M. Asta, J. Phys.: Condens. Matter **17**, 2197 (2005).
[19] M. Asta, V. Ozolins, and C. Woodward, JOM **53**, 16 (2001).
[20] C. Wolverton and D. Defontaine, Phys. Rev. B **49**, 8627 (1994).
[21] M. Asta, C. Wolverton, D. Defontaine, and H. Dreysse, Phys. Rev. B **44**, 4907 (1991).
[22] A. van der Ven, M. K. Aydinol, G. Ceder, G. Kresse, and J. Hafner, Phys. Rev. B **58**, 2975 (1998).
[23] C. Wolverton and A. Zunger, Phys. Rev. B **57**, 2242 (1998).
[24] A. Van de Walle and M. Asta, Metall. Mater. Trans. A **33**, 735 (2002).
[25] P. E. Blochi, Phys. Rev. B **50**, 17953 (1994).
[26] G. Kresse and J. Furthmuller, Comput. Mater. Sci. **6**, 15 (1996).
[27] J. P. Perdew, K. Burke, and Y. Wang, Phys. Rev. B **54**, 16533 (1996).
[28] A. I. Liechtenstein, V. I. Anisimov, and J. Zaane, Phys. Rev. B **52**, R5467 (1995).
[29] F. Zhou, M. Cococcioni, C. A. Marianetti, D. Morgan, and G. Ceder, Phys. Rev. B **70**, 235121 (2004).
[30] C. Wolverton and A. Zunger, Phys. Rev. Lett. **81**, 606 (1998).
[31] M. de Dompablo, A. Van der Ven, and G. Ceder, Phys. Rev. B **66**, 064112 (2002).
[32] A. Van der Ven and G. Ceder, Electrochem. Commun. **6**, 1045 (2004).
[33] Y. Hinuma, Y. S. Meng, K. S. Kang, and G. Ceder, Chem. Mater. **19**, 1790 (2007).
[34] P. D. Tepesch, G. D. Garbulsky, and G. Ceder, Phys. Rev. Lett. **74**, 2272 (1995).
[35] F. Zhou, T. Maxisch, and G. Ceder, Phys. Rev. Lett. **97**, 155704 (2006).
[36] Y. Hinuma, Y. S. Meng, and G. Ceder, Chem. Mater. **19**, 1790 (2007).
[37] G. Ceder, P. D. Tepesch, and A. F. Kohan, J. Electroceram. **1**, 15 (1997).
[38] A. van de Walle and G. Ceder, J. Phase Equilib. **23**, 348 (2002).
[39] J. Hubbard, Phys. Rev. B **17**, 494 (1978).
[40] D. de Fontaine, G. Ceder, and M. Asta, Nature (London) **343**, 544 (1990).
[41] D. de Fontaine, J. Phys.: Condens. Matter **A17**, L713 (1984).
[42] Q. Huang, M. L. Foo, R. A. Pascal, J. W. Lynn, B. H. Toby, T. He, H. W. Zandbergen, and R. J. Cava, Phys. Rev. B **70**, 184110 (2004).
[43] R. J. Balsys and R. L. Davis, Solid State Ionics **93**, 279 (1996).
[44] I. R. Mukhamedshin, H. Alloul, G. Collin, and N. Blanchard, Phys. Rev. Lett. **93**, 167601 (2004).
[45] H. X. Yang, C. J. Nie, Y. G. Shi, H. C. Yu, S. Ding, Y. L. Liu, D. Wu, N. L. Wang, and J. Q. Li, Solid State Commun. **134**, 403 (2005).
[46] I. R. Mukhamedshin, H. Alloul, G. Collin, and N. Blanchard, e-print arXiv:cond-mat/0703561.
[47] P. Carretta, M. Mariani, C. B. Azzoni, M. C. Mozzati, I. Bradaric, I. Savic, A. Feher, and J. Sebek, Phys. Rev. B **70**, 024409 (2004).
[48] J. Bobroff, G. Lang, H. Alloul, N. Blanchard, and G. Collin, Phys. Rev. Lett. **96**, 107201 (2006).
[49] G. Gasparovic, R. A. Ott, J. H. Cho, F. C. Chou, Y. Chu, J. W. Lynn, and Y. S. Lee, Phys. Rev. Lett. **96**, 046403 (2006).
[50] M. L. Foo, Y. Y. Wang, S. Watauchi, H. W. Zandbergen, T. He, R. J. Cava, and N. P. Ong, Phys. Rev. Lett. **92**, 247001 (2004).
[51] K. W. Lee and W. E. Pickett, Phys. Rev. Lett. **96**, 096403 (2006).
[52] D. J. Singh, Phys. Rev. B **61**, 013397 (2000).
[53] K. W. Lee and W. E. Pickett, J. Appl. Phys. **99**, 08P702 (2006).
[54] T. Motohashi, R. Ueda, E. Naujalis, T. Tojo, I. Terasaki, T. Atake, M. Karppinen, and H. Yamauchi, Phys. Rev. B **67**, 064406 (2003).
[55] J. Sugiyama and H. Itahara, Phys. Rev. B **67** 214420 (2003).
[56] L. M. Helme, A. T. Boothroyd, R. Coldea, D. Prabhakaran, D. A. Tennant, A. Hiess, and J. Kulda, Phys. Rev. Lett. **94**, 157206 (2005).
[57] G. J. Shu, A. Prodi, S. Y. Chu, Y. S. Lee, H. S. Sheu, and F. C. Chou, Phys. Rev. B **76**, 184115 (2007).

Downloaded 06 Jun 2011 to 137.110.115.65. Redistribution subject to AIP license or copyright; see http://jcp.aip.org/about/rights_and_permissions